The Simple Rectification to Cartesian Space of Folded Radial Velocities from Doppler Radar Sampling*

L. JAY MILLER, CARL G. MOHR AND ANDREW J. WEINHEIMER

*National Center for Atmospheric Research** Boulder, CO 80307*

(Manuscript received 5 September 1984, in final form 8 July 1985)

ABSTRACT

Periodic sampling of the Doppler radar return signal at the pulse repetition frequency causes measured velocities to be ambiguous (folded) when true meteorological velocities along the radial direction exceed the Nyquist or folding value. Furthermore, mean radial velocity estimates become more uncertain as the spatial variability of velocity increases or the returned signal strength decreases. These data have conventionally been prepared for such uses as multiple-Doppler radar wind synthesis by unfolding and editing them in the sampling domain (range–azimuth–elevation spherical coordinates).

An alternative method of locally (to the output grid point) unfolding the *unedited* radial velocities during their linear interpolation to a regular Cartesian grid is presented. The method preserves the spatial discontinuities of order twice the Nyquist value associated with velocity folding. A nondimensional velocity quality parameter is also computed which serves to identify interpolated values that contain too much variance to be reliable. Editing of radar data is thereby postponed until all radar data are mapped to the analysis coordinate system. This allows for iterative global unfolding and multiple-Doppler synthesis of complicated convective storm flow patterns. The resolution of folding in such flow fields may require more information than is usually available from single radar radial velocity fields in spherical coordinates. Further, the amount of data that must be subsequently manipulated is reduced about ten-fold in the process of interpolation.

1. Introduction

Radial velocities measured by Doppler radars are often interpolated to a regular (x, y, z) grid, especially when they are used in the multiple radar synthesis of three-dimensional wind fields. Although the processing of multiple radar data involves other steps such as the actual synthesis of three-dimensional winds using measurements from several viewing directions (e.g., Carbone et al., 1980), we have restricted this paper to the transformation of data from radar space to analysis space (interpolation), the removal of velocity ambiguities (unfolding), and the elimination of spurious values (thresholding). Common practice is to edit and unfold individual radar velocity measurements in the sampling space (range–azimuth–elevation; R, A, E) before interpolating them (e.g., Ray and Ziegler, 1977; Oye and Carbone, 1981). However, this step can be done after interpolation provided the remapping method preserves the statistical characteristics of the measured radial velocities and does not introduce any

biases in the interpolated values. Two especially important characteristics are the spatial discontinuities associated with folding of the radial velocities due to periodic sampling at the pulse repetition rate and the randomness of velocities when the backscattered signal strength indicates that only noise is present.

Most radar systems use the covariance or "pulse-pair" technique (e.g., Zrnić, 1977) to estimate the power-weighted average radial velocity within pulse volumes at several range locations along the pointing direction. When only noise is present in the backscattered return, this technique should give mean radial velocities that are uniformly distributed from $-V_n$ to V_n (the Nyquist co-interval) where V_n is the folding or Nyquist velocity. Unknown biases in the radial velocity processor can sometimes corrupt the noise distribution, but it is usually nearly uniform with a few preferential estimates occasionally occurring.

When the magnitude of the true meteorological radial velocity within a pulse volume exceeds V_n, sampling the return signal at the pulse repetition rate will cause estimates of Doppler velocity to be ambiguous or folded (e.g., Doviak et al., 1978). When this happens an integer multiple of twice the Nyquist velocity must be added to the measured pulse-volume average value to remove this ambiguity (Ray and Ziegler, 1977). Folding therefore represents an artificial and identifi-

able spatial discontinuity of order $2V_n$ in the radial velocity. If the discontinuity is not handled properly when aliased data are transformed to a regular xyz-grid, the velocity estimates cannot be correctly unfolded after interpolation.

The three-dimensional interpolation scheme developed by Mohr and Vaughan (1979) has been modified to include range averaging and local velocity unfolding. They determined the grid point value by a three-dimensional linear interpolation of eight measured values from two consecutive range locations along the four beams (two azimuths from each of two elevation scans) surrounding the grid point. All these data are usually obtained within 10–15 s (30–40 s in extreme cases of large azimuthal sectors) even though the scan of the entire volume of interest may take 2–3 min. Radar data that contain ambiguous measurements can be interpolated with this method *without first unfolding them*

in radar sampling space since the extension we propose preserves the original spatial discontinuities associated with folding. Further, this local unfolding technique applied to uniformly distributed noise estimates results in interpolated noise that remains nearly uniform with almost the same variability as the original distribution. The algorithm is discussed and the application of this procedure to a folded velocity field is presented. The advantages and cautions associated with this technique are also discussed.

2. Rectification of folded radial velocities

An example of radial velocities measured at an elevation angle of 9.5° by the NCAR/FOF (Field Observing Facility) CP-2 10-cm radar on 2 August during the 1981 Cooperative Convective Precipitation Experiment (CCOPE; Knight, 1982) in southeastern Mon-
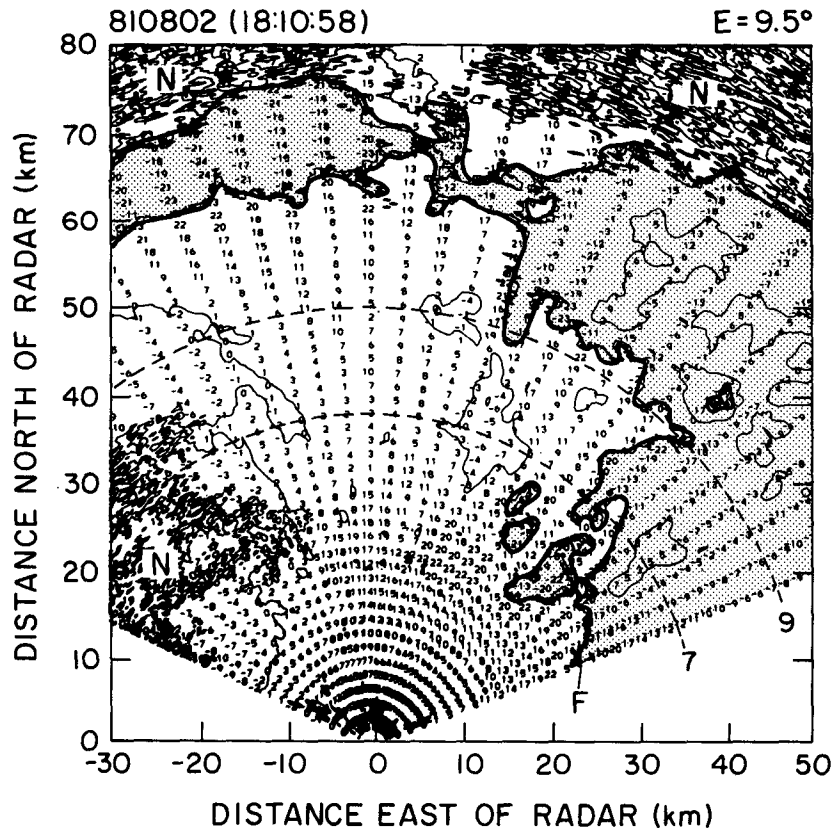

FIG. 1. Horizontal projection of measured radial velocities at an elevation angle of 9.5° from CP-2. These data were obtained on 2 August 1981 during the CCOPE field program in southeastern Montana. Numbers at every eighth gate along every sixth ray represent the magnitude of the radial velocity (positive values indicate motion away from the radar), with contours drawn at −25, 0 and 25 m s^{-1}. The bold line (F) indicates the position of the local discontinuity associated with folding. Regions of ambiguous or folded (about the Nyquist velocity of 25.6 m s^{-1}) velocities are shaded. Noisy estimates (N) exist to the northwest and also beyond about 70 km north of the radar. Ranges where the 7 and 9 km horizontal planes pass through this elevation surface are shown by dashed arcs.

tana is shown in Fig. 1. These data are part of the storm-volume scan from 1809:09 to 1812:32 (Mountain Daylight Time) that will be used to demonstrate the proposed technique. The storm was sampled every 200 m, 0.7° and 1° in range, azimuth, and elevation, respectively. The local discontinuity associated with folding is marked with a bold line. At locations away from the fold discontinuity the radial velocity field is again continuous, though perhaps ambiguous. Shaded regions in the figure contain ambiguous velocities while noise estimates exist beyond about 70 km to the north and in a patch northwest of the radar. Figure 2 shows these data after velocities have been unfolded in radar space using conventional methods (e.g., Oye and Carbone, 1981). In this example, noisy estimates (those mean values from low signal-to-noise power ratio regions or from broad velocity spectra) are retained though they could have been easily removed. In Section 4 we will compare interpolations of folded (Fig. 1) and unfolded (Fig. 2) values at 7 and 9 km (dashed arcs) to demonstrate that the same results can be obtained using the proposed alternative method.

Conventional editing and unfolding steps can be postponed until after interpolation so long as poor estimates of velocity and folding can still be identified. The idea is to designate a local velocity at each (x, y, z) point and to offset all velocities that affect this point so that they lie within the ambiguous velocity interval of this initial estimate prior to interpolation. This is done independently at each interpolation grid point and only represents a local resolution of velocity folding. Interpolated velocities which are folded must be subsequently de-aliased in Cartesian space using global techniques.

The true (unfolded) radial velocity U at a (R, A, E) measurement point is

$$U = V + \kappa V_a; \quad \kappa = 0, \pm 1, \pm 2, \cdots \quad (1)$$

where V is the measured quantity which may be aliased and is subject to measurement error, $V_a = 2V_n$ is the ambiguous velocity interval, and κ is the integer factor needed to remove Nyquist folding ambiguities from V. When the measured velocity differs by more than V_n from the value expected at the grid point, the integer folding factor in Eq. (1) is nonzero and can be approximated by
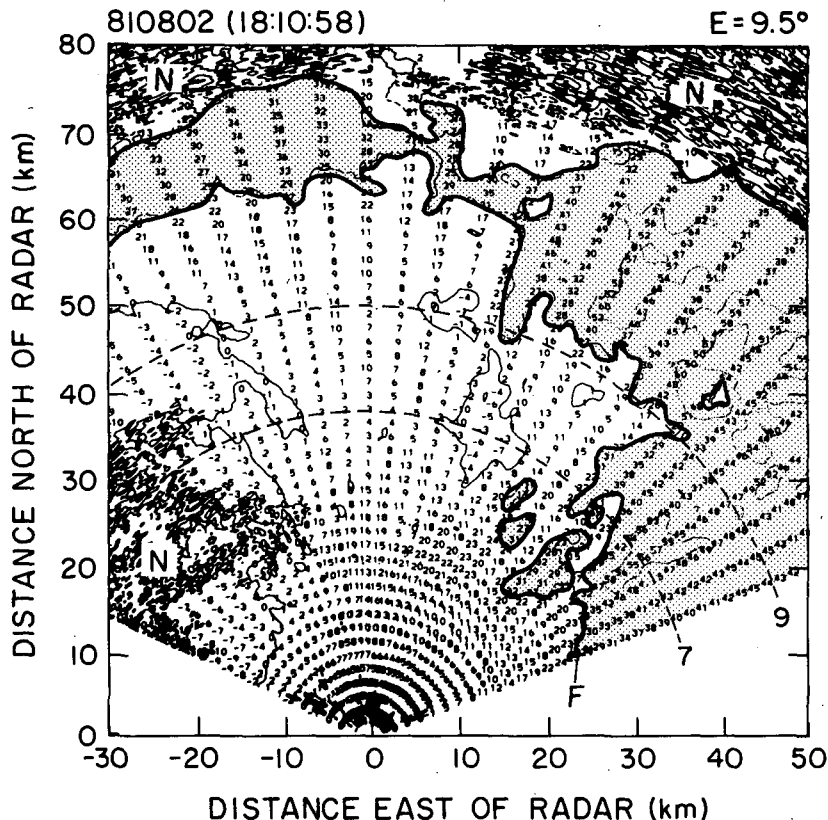

FIG. 2. Radial velocities shown in Fig. 1 after they have been unfolded in radar space. Areas where velocities have been de-aliased are shaded. An additional contour at 51.2 m s⁻¹ has been added. This corresponds to the zero contour in the ambiguous zone in Fig. 1.

$$K = \frac{U_e - V}{V_a}, \qquad (2a)$$

where U_e is a preliminary estimate of the true radial velocity (U) at the (x, y, z) point. The appropriate integer unfolding factor is determined by

$$\kappa = \begin{cases} \text{INT}(K + 0.5), & \text{if } K \geq 0 \\ \text{INT}(K - 0.5), & \text{if } K < 0, \end{cases} \qquad (2b)$$

where INT represents truncation toward zero. The quantity U_e is arbitrarily set to one of the measured input values in the neighborhood of the (x, y, z) point, and the remaining contributing values are forced into the ambiguous velocity interval centered on U_e using Eqs. (1) and (2). Strictly this operation does not represent complete unfolding, but temporary removal of a discontinuity that would result in biased estimates when interpolation to grid points is performed. To completely unfold or de-alias the velocities, the addition or subtraction of another integer multiple of V_a may still be needed after interpolation. Henceforth, we will refer to the removal of the folding discontinuity within the population of input measurements contributing to the estimate at each (x, y, z) point as local unfolding or more simply as "unfolding."

Since U_e comes from the population of input samples which are contained within the Nyquist co-interval (unless they have been previously unfolded), the values of κ determined by Eq. (2) will be -1, 0, or $+1$. *It is assumed that no true velocity is more than V_n from the reference velocity.* This is equivalent to assuming that the largest possible physical gradients of radial velocity that can occur within the sampling cell surrounding the Cartesian grid point are $V_n/(M-1)\Delta R$ in range, $V_n/R\Delta A$ cos$E$ in azimuth, and $V_n/R\Delta E$ in elevation, where ΔR, ΔA and ΔE are the respective sampling increments. The sampling cell consists of M range (R) gates and four adjacent beams, two in azimuth (A) and two in elevation (E). Spatial gradients across the sampling cell larger than these will cause the true radial velocities to be spread over more than one V_a interval, leading to the requirement that some values of κ exceed unity. In this event, which is uncommon provided the Nyquist velocity is large (about 25 m s^{-1}) and radar (R, A, E) sampling locations are closely spaced (less than about 1 km), the algorithm will obviously fail to interpolate an unbiased velocity value.

Radar velocity measurements from a range slab of thickness M gates centered at slant range R to the interpolation xyz-grid point are range-averaged to obtain estimates at each of four azimuth-elevation locations surrounding the xyz-grid point:

$$\hat{U}(A_j, E_k) = \sum_{m=1}^{M} U_m/M,$$

where the U_m have been "unfolded" according to Eqs.

(1) and (2). This step is done to approximately equalize the sampling increments in the range and cross-beam directions and is not intended to represent complete filtering that may be required. The quantities A_j and E_k represent the respective azimuth and elevation angles of the beams. A caret denotes either range-averaged or xyz-grid values, and quantities without a caret represent either measured or "unfolded" velocities at radar sampling locations. The geometry of the angular sampling cell at the range of the xyz-grid point and interpolation are illustrated in Fig. 3. Following Mohr and Vaughan (1979), these range-averaged data are bilinearly interpolated using

$$\hat{U}(A, E) = \left(\frac{E_{k+1} - E}{\Delta E}\right)$$

$$\times \left[\hat{U}_j\left(\frac{A_{j+1} - A}{\Delta A}\right) + \hat{U}_{j+1}\left(\frac{A - A_j}{\Delta A}\right)\right]_k + \left(\frac{E - E_k}{\Delta E}\right)$$

$$\times \left[\hat{U}_j\left(\frac{A_{j+1} - A}{\Delta A}\right) + \hat{U}_{j+1}\left(\frac{A - A_j}{\Delta A}\right)\right]_{k+1}, \quad (3)$$

where $\Delta E = E_{k+1} - E_k$, $\Delta A = A_{j+1} - A_j$. The terms in brackets represent linear interpolations along azimuth at the k and $k + 1$ elevation levels. Combining Eqs. (1) and (3), in abbreviated form the "unfolded" and interpolated radial velocity becomes

$$\hat{U}(x, y, z) = \sum_{A,E} (wV)_{jk} + V_a \sum_{A,E} (w\kappa)_{jk}. \qquad (4)$$

The first term on the right is the geometrically weighted sum of measured values, while the second term represents a weighted folding factor to correct for bias that would result if measured values were not locally unfolded before interpolation. The quantity w is the geometric weighting factor associated with each (A_j, E_k) location in Eq. (3). The values of κ in Eq. (4) are the
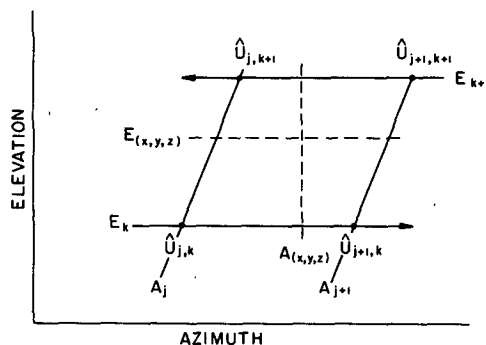
FIG. 3. The geometry of the sampling cell and bilinear interpolation along a constant range surface passing through the Cartesian grid point (x, y, z). The $\hat{U}_{jk}$ represent the averages of M range gate measurements centered at $R(x, y, z)$ and located at the four radar beams left and right, above and below the point $A(x, y, z)$, $E(x, y, z)$.

ones that must be used to remove the local discontinuity from the measured velocities.

The form of the weighting function to be used in Eq. (4) for interpolating radar information to a regular Cartesian grid is usually a matter of personal preference. We choose the linear weighting and range averaging presented in Eq. (3); other distance weighting schemes such as the Cressman method (e.g., Ray et al., 1975) could also be used. All such schemes assign a distance-weighted average value to the grid point, where the weight decreases rapidly as the distance from the grid point increases or else only estimates within some small radius of the grid point are used. It is not our intent to debate the virtues of all such schemes; however, if the method employed uses values only in proximity to the output grid point, the discontinuity associated with folding can be removed and then the weighting applied in the way we present. That is, they can be interpolated without prior radar-space editing.

Figure 4 illustrates the results of interpolating the folded radial velocity field (shown in Fig. 1) at two levels in the storm using the methodology that we propose. These horizontal planes at 7 (Fig. 4a) and 9 km (Fig. 4b) intersect the elevation plane in Fig. 1 at the dashed arcs. The boundary of folded radial velocities in the southeast portion of the grid is shown by a bold line, with shading indicating regions of ambiguous velocities as in Fig. 1. A zone of ambiguous velocities extends northward along the eastern portion of the grid as also seen in Fig. 1. The patch of noisy measurements northwest of the radar is also clearly replicated as evidenced by the many contours in the western portion of the domain. A time associated with each interpolation grid point is also obtained by applying the same linear interpolation scheme to the original observation times. In this way the multiple radar synthesis that includes advective corrections at Cartesian grid points as formulated by Gal-Chen (1982) can be utilized.

3. Quality of the interpolated velocities

Since the interpolation method is applied to all radar-measured velocities without prior editing, we need a way to determine the quality of the interpolated value. This measure can be used later in Cartesian space to reject unreliable velocities interpolated from radar measurements that are too noisy and to identify regions where local unfolding may have required a folding factor exceeding unity. When no signal is present covariance-measured radial velocities ideally have variance $\sigma_n^2 = V_n^2/3$, so that large local variability should tell us when interpolated values are coming from an input population dominated by noise. Further, large spatial gradients of the measured velocities should also lead to significant variability. When neither of these conditions exist, the spread of velocities should be much smaller. Thus we compare the sample variance var(U)

of "unfolded" velocities to be used in the interpolation with the expected value of σ_n^2 for white noise to determine the reliability of the interpolated velocity. A nondimensional velocity quality parameter

$$Q(x, y, z) = 1 - \mathrm{var}(U)/\sigma_n^2 \qquad (5)$$

is calculated. All measurements affecting a grid point estimate are locally unfolded using Eqs. (1) and (2) and then their corresponding variance var(U) is obtained.

The nondimensional velocity quality parameter Q is close to zero when all radial velocities are noise (see Appendix for the expected value and variance of Q when a noise population is unfolded), and it approaches unity as the spatial variability of the measured velocities decreases. Further, Q can become negative when the distribution of "unfolded" measurements is more clustered toward its extreme values with fewer estimates near the center velocity. The parameter Q reflects variability from measurement errors in individual velocities as well as large spatial gradients in the true radial velocity field surrounding the interpolated grid point. It is, therefore, a better measure of the acceptability of grid point estimates than is the magnitude of the covariance function which is often used to determine reliability of individual measurements contributing to the interpolated estimate. More importantly, Q can be computed for all radar systems in the same way. Systems that do not record the magnitude of the covariance function instead flag the velocity as good or bad at the time of measurement (e.g., the bad data flag bit used in the NCAR/FOF 5 and 10 cm radars). Unfortunately, such procedures do not allow the data-user to decide if these values are acceptable for his purposes.

An example of the actual behavior of Q in a noise-only environment was determined by interpolating radial velocities from NCAR's CP-2 radar. The transmitter was intermittent for a short time on 11 July 1981 during CCOPE so that noise-only data could be recorded while the antenna was rotating and the processing system was still operating. This provided recorded data at spatial resolution typically associated with normal probing of severe convective storms. The frequency distribution of Q for interpolation at one horizontal level is shown in Fig. 5 (solid line histogram). It roughly obeys a Gaussian law with a nearly zero mean value and standard deviation of about 0.3 so that interpolated (signal) velocities appear to be acceptable when $Q > 0.6$. This can be seen also in the distribution of Q when both signal and noise are present (Fig. 5, dashed line histogram). The values to the right of 0.6 are definitely associated with signal since a value of $Q = 0.8$ corresponds to var(U) = 43.7 m^2 s^{-2} with noise variance $\sigma_n^2 = 218.4$ m^2 s^{-2} for this case. (The Nyquist velocity was 25.6 m s^{-1}).

A histogram of noise input velocities from a volume scan on 2 August 1981 (Fig. 1) is shown in Fig. 6a. The percent of the total number of values (3194) appearing
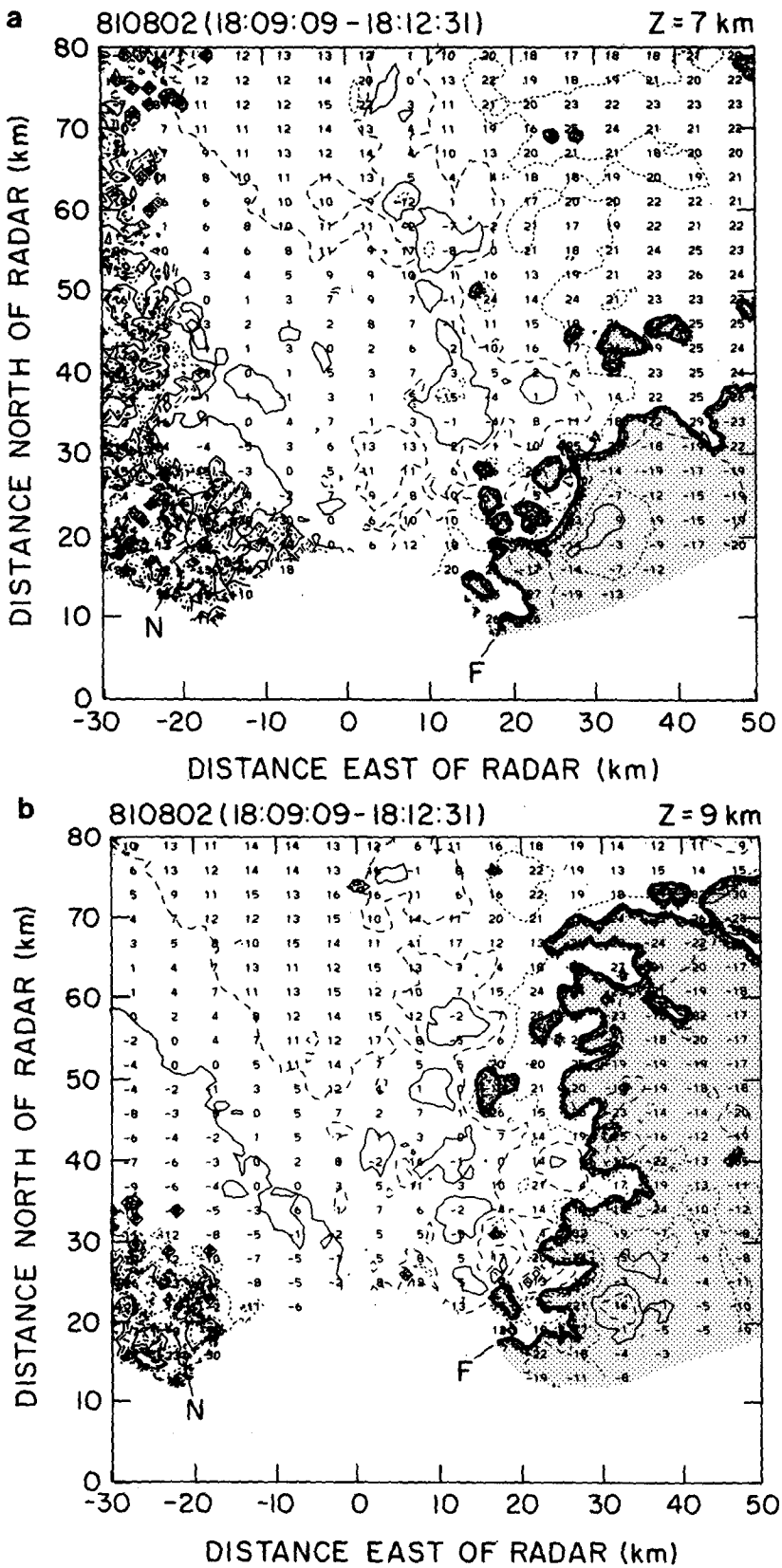
FIG. 4. Samples of unedited and interpolated (with local unfolding) radial velocities at (a) 7 km and (b) 9 km. These horizontal sections pass through the 9.5° elevation plane of Fig. 1 at the dashed arcs. Numbers represent the radial velocity at selected locations with contours drawn at 10 m s^{-1} intervals starting at -30 m s^{-1} in the repeating pattern: dashed, short-dashed and solid. The zero contour is solid. The bold line (F) marks the position of the local discontinuity caused by folding. The regions of ambiguous (folded) velocities are shaded. Noisy velocities (N) exist along the western portion of the grid.
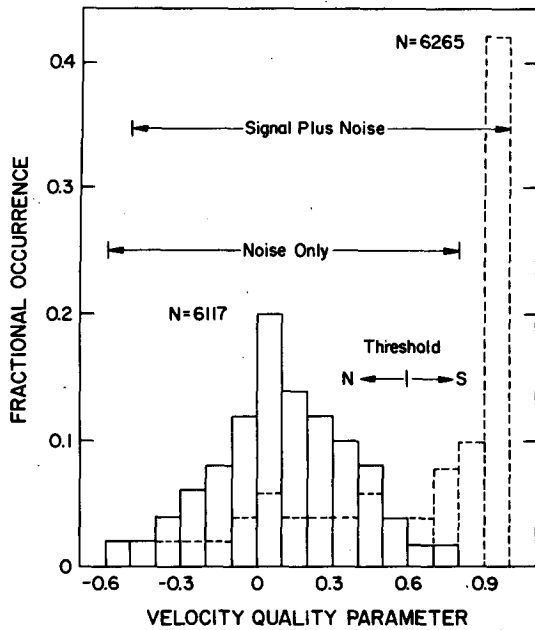
FIG. 5. Frequency distributions of velocity quality parameter for interpolated noise-only (solid) and signal-plus-noise (dashed) radial velocity fields. The numbers of values at this horizontal level (6 km above mean sea level) used to determine the distributions were 6117 and 6265, respectively. A value of 0.6 appears to adequately separate noise from signal.

in each of the bins of width 2 m s^{-1} is represented by the ordinate. The distribution is nearly uniform with sample mean of 0.01 m s^{-1} and standard deviation of 14.51 m s^{-1}, compared to theoretical values of 0.0 and 14.78 m s^{-1}, respectively. The distribution of inter-polated (with local unfolding) velocities corresponding to the noise-only input velocities in Fig. 6a is shown in Fig. 6b. Since the reference velocity used for local unfolding is itself equally likely to occur anywhere within the ambiguous velocity interval, the effect of interpolation with unfolding is to create local Gaussian populations having an expected value of U_e and con-ditional variance equal to that of $\hat{U}$ for a given U_e. The distribution of $\hat{U}$ is then a convolution of this (relatively narrow) Gaussian with the original uniform distribu-tion (Rohatgi, 1976). The tendency for more values to be concentrated near zero is mostly a result of con-volving a Gaussian distribution whose width depends on the number of original measurements used in the interpolation with the *actual* distribution of velocities coming from the radar processor.

If no local unfolding were invoked the distribution of velocities would look like the one shown in Fig. 6c. If the radial velocities come from statistically similar populations having zero mean and equal variance σ_n^2, the variance of the grid point estimate is

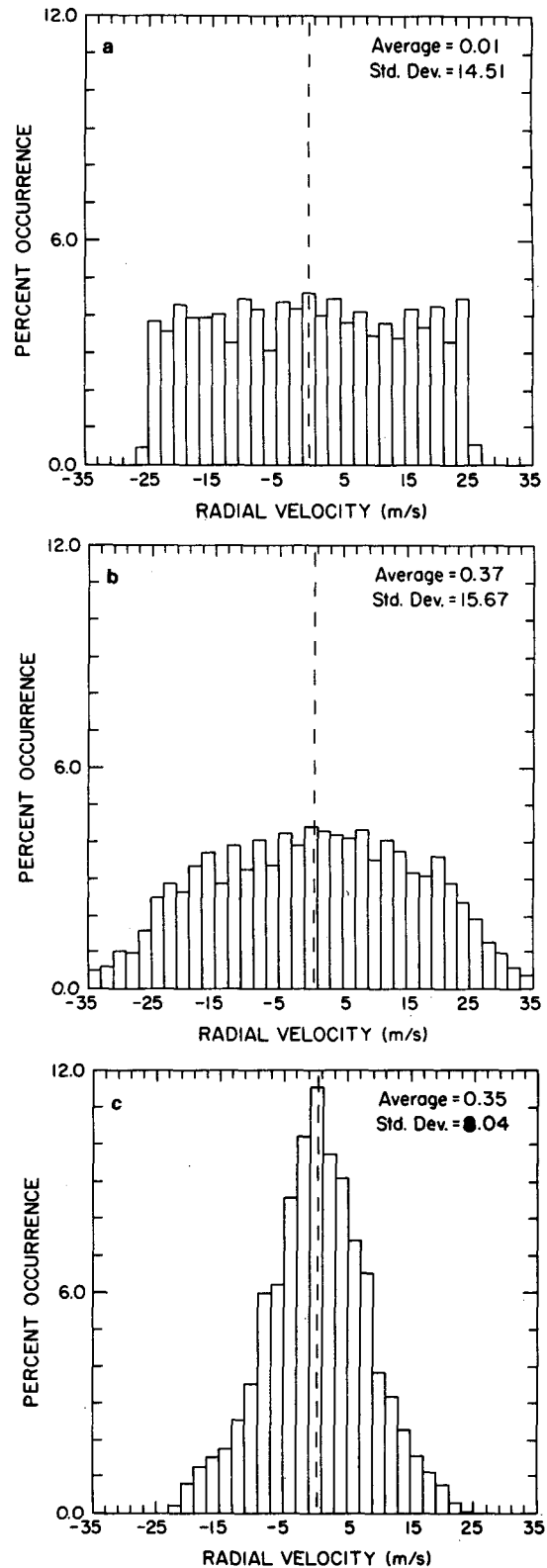$$\sigma^2(\hat{U}) = \sigma_n^2 \frac{\sum w_{jk}^2}{M},$$

FIG. 6. Frequency distributions of radial velocities for "noise-only" (i.e., Q less than 0.5) portions of the 2 August radar scan volume presented in Figs. 1, 2 and 4: (a) input, (b) interpolated with local unfolding, and (c) interpolated without local unfolding. The average

where the quantities w_{jk} are the geometric weighting factors in Eq. (3). If the grid point should happen to coincide with an original sample location, all the weights except one are zero. If, however, the grid point is equidistant from all four sample locations (see Fig. 3), the sum of squares of weights is 0.25. Since all values of A, E are equally likely to occur, the expected value of $\Sigma\ w_{jk}^2$ is its areal average of 4/9. Three gates were used so the expected variance is $0.15\sigma_n^2$ or a standard deviation of 5.7 m s^{-1} compared to the observed value of 8.04 m s^{-1} (Fig. 6c). As can be seen the distribution of interpolated (with local unfolding, Fig. 6b) noise-only measurements is clearly "noiselike" and is similar to the one found in radar space (Fig. 6a). The importance of the local unfolding is further evidenced by noting the character of the contours in the western portion of Fig. 4a and contrasting that with what would happen if no local unfolding were invoked during interpolation (Fig. 6c). Some of the chaotic character would be lost.

4. Comparison with conventional methods

All radial velocities except noisy ones (as determined by the bad data flag bit) were carefully unfolded in radar space and then interpolated using the linear method with three-gate smoothing, but with no additional local unfolding. Examples of these data are shown in Fig. 7. Shaded regions in the eastern portion of the grid where velocities were originally ambiguous are now unfolded. Noisy estimates in the western portion were interpolated with local unfolding to replicate the effects discussed in Section 3.

For comparison, unedited original measurements such as those shown in Fig. 1 were interpolated with local unfolding and then unfolded in Cartesian space (Fig. 8), using global techniques described by Mohr and Miller (1983). These data were also thresholded on the velocity quality parameter ($Q > 0.6$) to eliminate the noisy portion. At grid locations outside regions of noise the average difference between velocity estimates derived by conventional methods and our method was 0.05 m s^{-1} with a standard deviation of only 0.11 m s^{-1}.

To further substantiate this equality of methods, we constructed several scatter plots to show point-by-point comparisons of velocities derived by conventional methods with those obtained by the proposed method. The following radial velocity fields were created:

VGUF—velocities were unfolded in radar space and then interpolated with no additional unfolding,

VNUF—unedited velocities were interpolated with local unfolding,

VLUF —the field VNUF was unfolded in Cartesian space,

VBIA —unedited velocities were interpolated without local unfolding,

VGTH—the field VGUF was thresholded on Q, and

VLTH —the field VLUF was thresholded on Q.

Figure 9a shows a scatter plot of the conventional method velocity (VGUF) along the abscissa versus the interpolated with local unfolding velocity (VNUF). There are two regression lines of VNUF that are offset by $V_a = 51.2$ m s^{-1} above and below (or right and left of) the one-to-one line. These represent values that need to be unfolded in Cartesian space, while values along the one-to-one line were never ambiguous in the first place. These velocities (VNUF) are shown in Fig. 9b after unfolding has been accomplished in Cartesian space. The few points that do not lie along the one-to-one line are from the noisy regions, as seen in Fig. 9c where these values have been eliminated by thresholding on Q. Note the small improvement in the correlation coefficient from $r = 0.998$ in Fig. 9b to $r = 1.000$ in Fig. 9c indicating that both methods are producing identical results in regions of usable data.

Contrast these results with the ones in Fig. 10 where unedited velocities were interpolated without local unfolding. The shaded area indicates regions where velocities cannot be unfolded by the addition or subtraction of any integer multiple of the ambiguous velocity. This is further demonstrated in Fig. 11 where these biased velocities (VBIA) are plotted against the conventional-method velocities (VGUF). The vertical scatter of VBIA near the Nyquist velocity typifies the amount of bias that occurred. The large scatter near the negative Nyquist is also from biasing as well as from noisy values. Although the bias in these velocities cannot be removed, all these interpolated velocity values can be eliminated by thresholding on the velocity quality parameter computed using unedited input measurements.

5. Concluding remarks

We have discussed a way of rectifying folded velocity measurements taken in radar sampling space to regular (x, y, z) analysis space. These locally unfolded and interpolated velocities can then be globally unfolded using techniques described by Mohr and Miller (1983). Noisy data are eliminated and remaining velocities are unfolded using the interactive software package CEDRIC (Mohr and Miller, 1983). This procedure has been shown to give results identical to those using more conventional approaches.

Two main advantages of not editing radial velocities until after interpolation are 1) the amount of radar data that must be subsequently manipulated is reduced by a factor of ten to twenty; and 2) all the data from

---

value is marked by a vertical dashed line. Each bin of width 2 m s^{-1} designates the percent of all velocities (total of 3194) that occurred within the bin. The average value and standard deviation of the distribution is shown in the upper right hand corner.
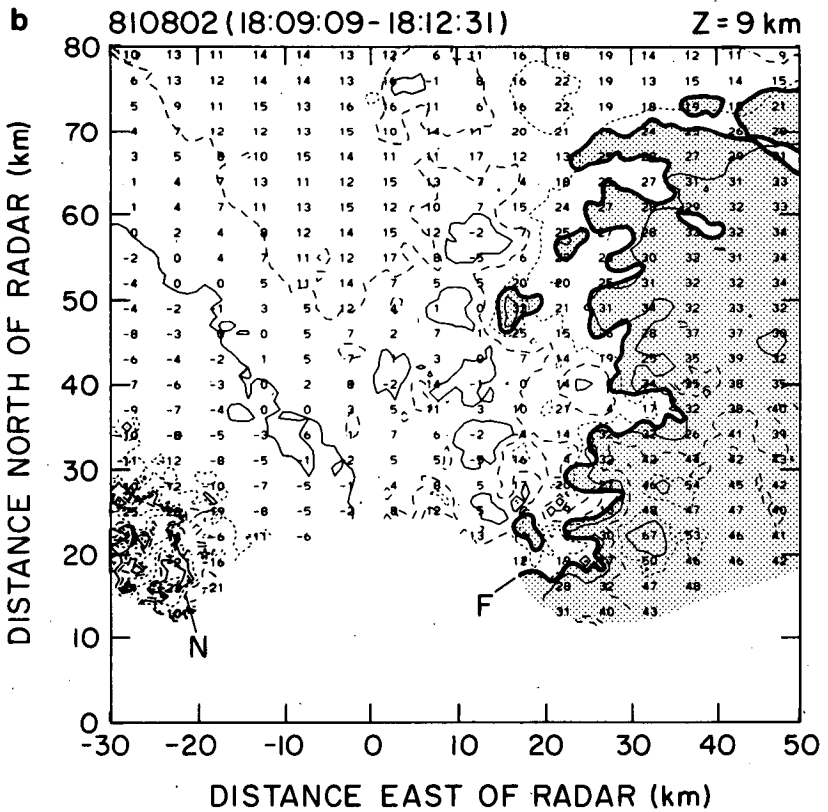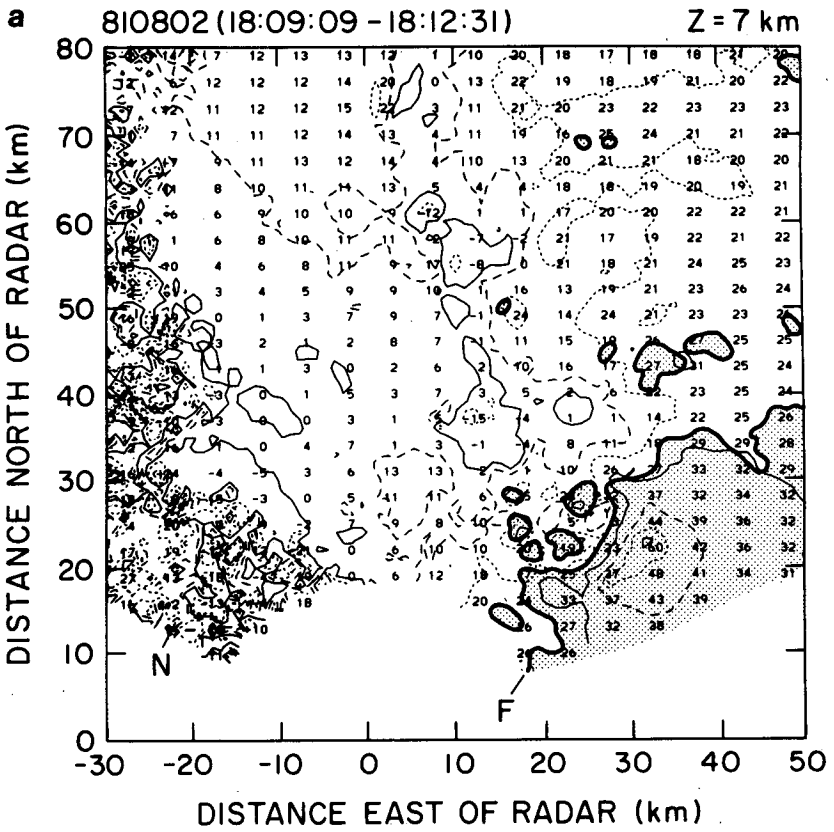
FIG. 7. Radial velocities at (a) 7 and (b) 9 km that were unfolded in radar space before they were interpolated. This format is identical to that given in Fig. 4. Additional contours are drawn at 30 m s^{-1} (solid), 40 m s^{-1} (dashed), 50 m s^{-1} (short-dashed), and 60 m s^{-1} (solid).
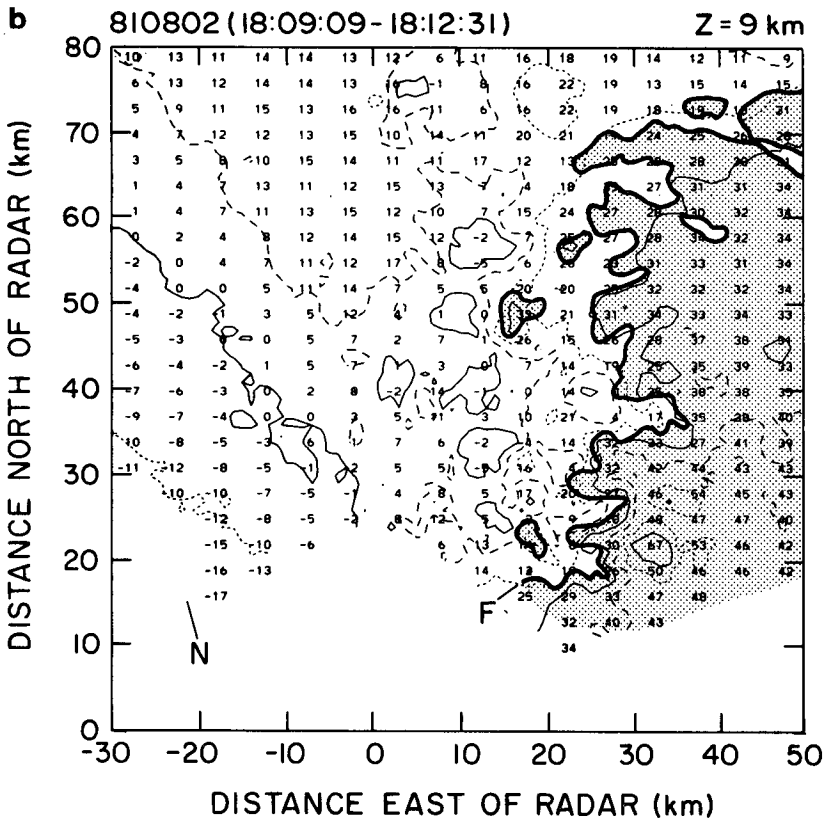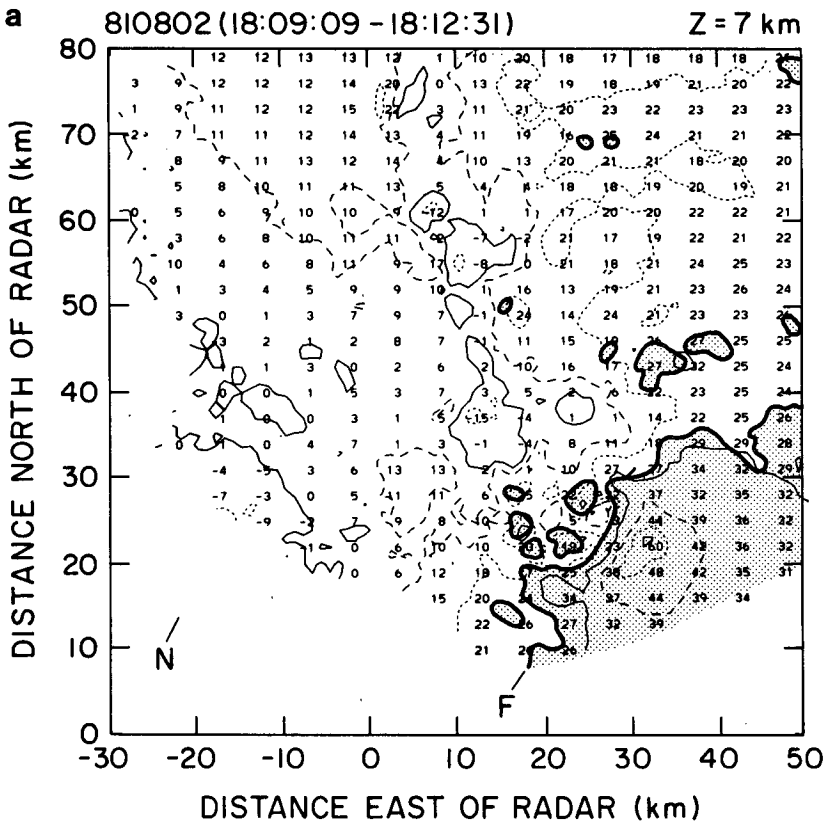
FIG. 8. Interpolated (with local unfolding) velocities shown in Fig. 4 that were unfolded in Cartesian space and thresholded on the quality parameter (Q greater than 0.6). Additional contours have been added as in Fig. 7. Compare these fields with those in Fig. 7.
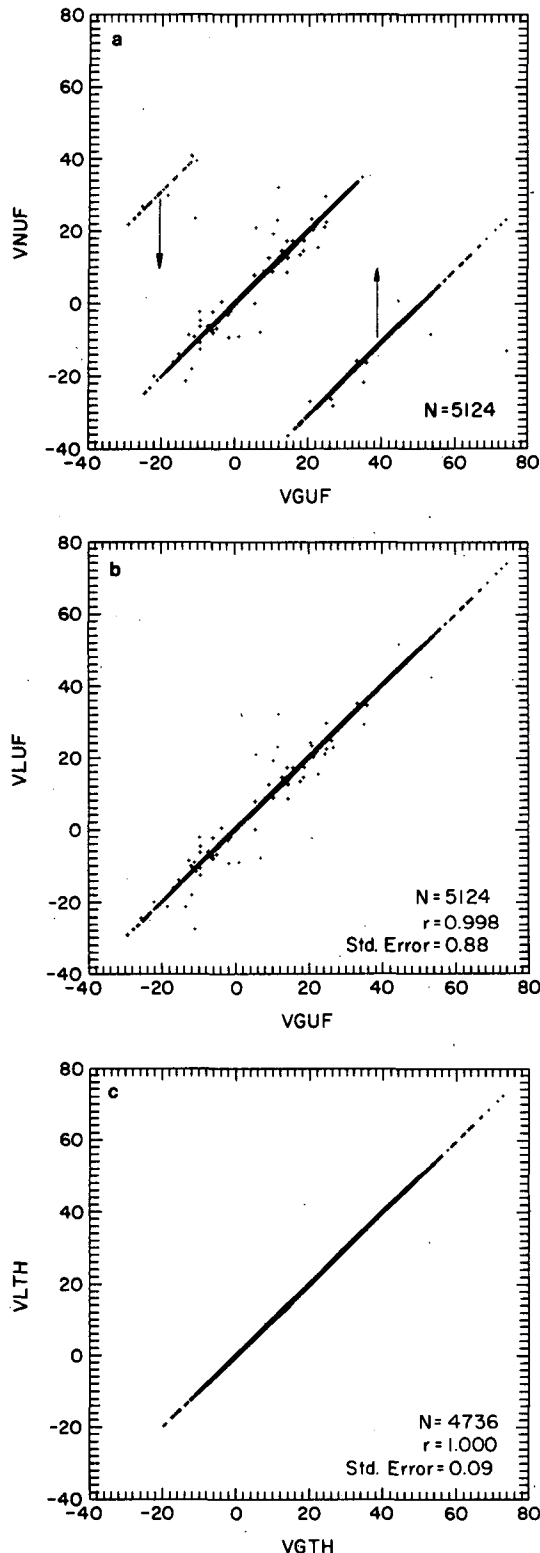
different radars are located at common grid points, thereby facilitating interactive global unfolding and multiple radar wind synthesis attempts of difficult cases. When adjacent true velocity values differ by more than twice the Nyquist velocity, the local unfolding-interpolation scheme will fail to interpolate a correct grid point estimate. Application of Eqs. (1) and (2) would give a folding factor of one, rather than the required two or more. The interpolated value would therefore be incorrect.

For a large severe storm there may be as many as 500–1000 range gates per beam, 100–200 beams per elevation sweep and 15–20 sweeps per storm volume or about $1-4 \times 10^6$ original sampling points per storm volume. These are typically interpolated to about 100 $\times$ 100 grid points at 15–18 vertical levels, or 1.5–1.8 $(\times 10^5)$ values. Large radar data bases such as the one from the CCOPE Doppler radar network can be written to mass storage devices (e.g., the terabit memory system at NCAR) where they can be processed using a batch version of this interpolation procedure (Mohr et al., 1981) on the CRAY-1A computer. Most of these radar measurements can be interpolated without prior radar-space editing and written to tape for transport to smaller machines such as a VAX 11/780 computer where the results can be edited and synthesized in Cartesian analysis space. This means that about one-tenth as many magnetic tapes must be handled, and most if not all of the data needed for a case study can reside on disk in the smaller machine.

Many times there is insufficient information available from a single radar to unambiguously unfold all the measured velocities. If the computation-intensive step of interpolation does not have to be repeated, preliminary unfolding and synthesis can be attempted. Incompatibilities between radars will usually show up as physically impossible resultant vector winds so that the offending values of radial velocity can then be unfolded in a different way and resynthesized. Furthermore, since most meteorologists are more accustomed to working with data on constant height surfaces rather than constant elevation angle surfaces (radar spherical coordinates), Cartesian space is a more comfortable framework for manipulating the data base and arriving at believable results. Measurements can be transformed without radar space editing in most cases so that the majority of the data processing can be delayed until all radar estimates are organized onto a common (for all radars) grid where editing is less tedious and time-consuming.

FIG. 9. Scatter plots of radial velocities that were unfolded in radar space and then interpolated (VGUF) versus (a) VNUF—locally unfolded during interpolation and (b) VLUF—unfolded VNUF in Cartesian space. The directions of movement of (VGUF, VNUF) pairs when VNUF is unfolded are marked by arrows in (a). VGTH was produced by thresholding VGUF on the velocity quality parameter and is plotted versus (c) VLTH—thresholded VLUF on quality parameter. The number of points (N), linear regression coefficient (r), and standard error [defined as $\sigma_y (1 - r^2)^{1/2}$, where σ_y is the ordinate] are marked in the lower right-hand corner.
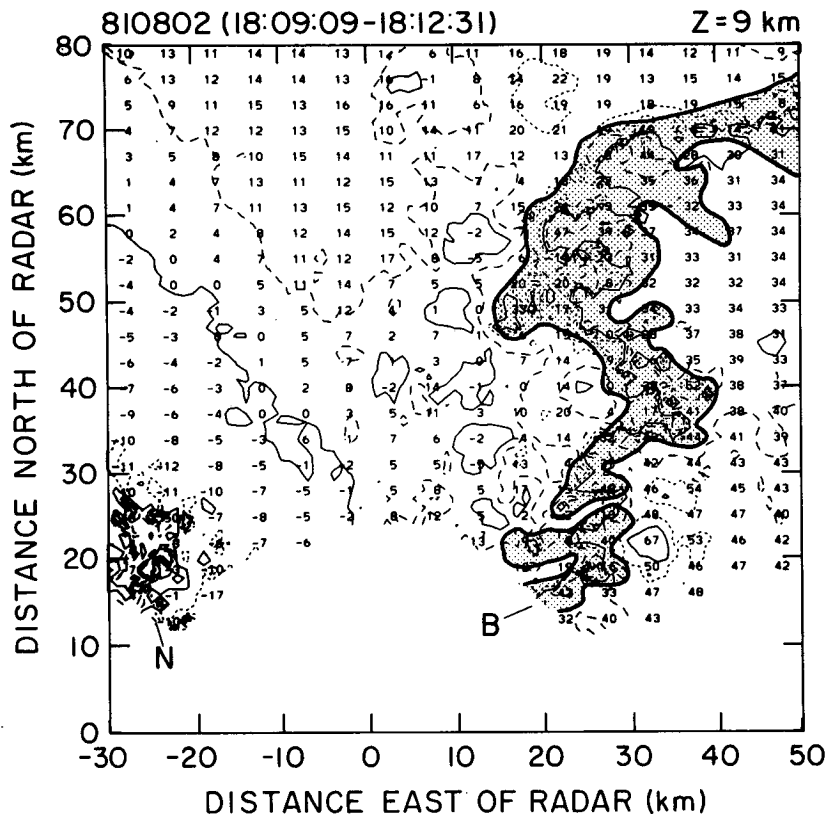
FIG. 10. Biased velocities that result when unedited and folded velocities are interpolated without invoking the local unfold algorithm. These data were then unfolded using the velocities in Fig. 7b as references. The shaded region surrounding the fold discontinuity contains biased velocities; that is, they cannot be unfolded to agree with Fig. 7b by the addition or subtraction of integer multiples of the ambiguous velocity, V_a.
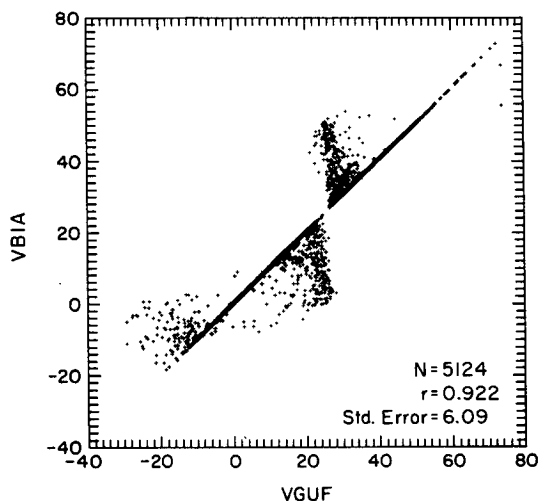

FIG. 11. As in Fig. 9 except VGUF versus VBIA— biased velocities of Fig. 10. This scatter plot clearly shows biasing in the grid point estimates that cannot be removed. However, those values that are biased can be eliminated from the dataset by thresholding on the velocity quality parameter.

technical staff in the maintenance and operation of the CP-2 radar. The success of the CCOPE experiment would not have been possible without the dedication of these technicians and engineers.

APPENDIX

Behavior of the Variance and Nondimensional Velocity Quality Parameter

In this appendix we consider the behavior of the variance [var(U)] and nondimensional velocity quality parameter (Q) in Eq. (5) when all radial velocity measurements are random noise. This is of fundamental importance since we calculate these statistics at each grid point and use their values to discriminate against interpolated velocities coming from regions of noise. The applicability of this exercise is limited, however, by the extent to which the pulse-pair processor is not ideal and does not yield a uniform distribution of output velocities in noise.

When no return signal is present, covariance-determined velocities will ideally be distributed uniformly

from $-V_n$ to V_n, and thus will have a zero mean and variance $\sigma_n{}^2 = V_n{}^2/3$. However, the unfolding of such a distribution to a reference velocity that is a sample from the population results in a variance somewhat smaller than $\sigma_n{}^2$. The velocity notation used in the main body of the paper is retained: at radar sampling locations V_i and U_i represent measured and unfolded velocities, respectively. The local mean value of the unfolded velocities is

$$\bar{U} = \frac{\sum U_i}{I}, \tag{A1}$$

with variance [$Z = \text{var}(U)$ in Eq. (5)]

$$Z = \frac{\sum (U_i - \bar{U})^2}{I - 1}. \tag{A2}$$

The expected value of Z for a uniform noise distribution is derived from the conditional probability density for the unfolded velocities U_i, given that a reference velocity $V_1 = v_1$ has been chosen. For $i \neq 1$, the U_i will be uniformly distributed over a range of $2V_n$ centered at v_1. The conditional probability density of the $U_i(i \neq 1)$ is

$$p_{U_i|V_i}(u_i|v_1) = \begin{cases} \dfrac{1}{2V_n}, & v_1 - V_n < u_i < v_1 + V_n \\ 0, & \text{otherwise.} \end{cases} \tag{A3}$$

Further, for $i = 1$ the unfolded velocity will certainly be v_1, given that $V_1 = v_1$:

$$p_{U_1|V_1}(u_1|v_1) = \delta(u_1 - v_1), \tag{A4}$$

where δ is the Dirac delta function. The conditional expectation or mean of each of the U_i is v_1:

$$E_c[U_i] = \int du_i u_i p_{U_i|V_i}(u_i|v_1)$$

$$= v_1. \tag{A5}$$

The conditional expectation of Z may be expressed in terms of the conditional variances of the U_i given by

$$E_c[(U_i - v_1)^2] = \begin{cases} \sigma_n{}^2, & i \neq 1 \\ 0, & i = 1. \end{cases} \tag{A6}$$

Then by taking steps identical to those in the derivation of the expected value of a sample variance (e.g., Bendat and Piersol, 1971), it follows that

$$E_c[Z] = \frac{I - 1}{I} \sigma_n{}^2. \tag{A7}$$

(This Z is actually not a sample estimate of variance in the usual sense, because the values of U_i do not constitute a random sample of a single random variable, U_1 being distributed differently than the other U_i.) From the definition of the velocity quality parameter in Eq. (5), the expected value of Q becomes

$$E_c[Q] = 1 - E_c[Z]/\sigma_n{}^2$$

$$= \frac{1}{I}. \tag{A8}$$

This will be near zero for most practical choices of I ($I = 12$ for 3-gate range averaging).

In order to distinguish between signal and noise using the parameter Q, it is important that the variance of Q in noise not be too large. Otherwise, a significant number of values of Q in noise, which are expected to be near zero, may actually be near unity, as they are for signal. The conditional variance of Q, $\text{var}_c[Q]$, may be shown to be

$$\text{var}_c[Q] = \frac{4}{5(I - 1)} \left(1 + \frac{1}{2I} - \frac{4}{I^2}\right)$$

$$\approx \frac{4}{5I}. \tag{A9}$$

This indicates that the reliability of Q as a discriminator against noise is increased by increasing the number of samples I going into each grid point estimate.

REFERENCES

Bendat, J. S., and A. G. Piersol, 1971: Random Data: Analysis and Measurement Procedures, Wiley-Interscience, 407 pp.

Carbone, R. E., F. I. Harris, P. H. Hildebrand, R. A. Kropfli, L. J. Miller, W. Moniger, R. G. Strauch, R. J. Doviak, K. W. Johnson, S. P. Nelson, P. S. Ray and M. Gilet, 1980: The multiple Doppler radar workshop, November 1979. Bull. Amer. Meteor. Soc., 61, 1169–1203.

Doviak, R. J., D. Sirmans, D. Zrnić and G. B. Walker, 1978: Considerations for pulse-Doppler radar observations of severe thunderstorms. J. Appl. Meteor., 17, 189–205.

Gal-Chen, Tzvi, 1982: Errors in fixed and moving frames of references: Applications for conventional and Doppler radar analysis. J. Atmos. Sci., 39, 2279–2300.

Knight, C. A. (Ed.), 1982: The Cooperative Convective Precipitation Experiment (CCOPE), 18 May–7 August 1981. Bull. Amer. Meteor. Soc., 63, 386–398.

Mohr, C. G., and L. J. Miller, 1983: CEDRIC—A software package for Cartesian space editing, synthesis and display of radar fields under interactive control. Preprints, 21st Conf. on Radar Meteorology, Boston, Amer. Meteor. Soc., 569–574.

——, and R. L. Vaughan, 1979: An economical procedure for Cartesian interpolation and display of reflectivity factor data in three-dimensional space. J. Appl. Meteor., 18, 661–670.

——, L. J. Miller and R. L. Vaughan, 1981: An interactive software package for the rectification of radar data to three-dimensional Cartesian coordinates. Preprints, 20th Conf. on Radar Meteorology, Boston, Amer. Meteor. Soc., 690–695.

Oye, R., and R. Carbone, 1981: Interactive Doppler editing software. Preprints, 20th Conf. on Radar Meteorology, Boston, Amer. Meteor. Soc., 683–689.

Ray, P. S., and C. Ziegler, 1977: De-aliasing first-moment Doppler estimates. J. Appl. Meteor., 16, 563–564.

——, R. J. Doviak, G. B. Walker, D. Sirmans, J. Carter and B. Bumgarner, 1975: Dual-Doppler observations of a tornadic storm. J. Appl. Meteor., 14, 1521–1530.

Rohatgi, V. K., 1976: An Introduction to Probability Theory and Mathematical Statistics, Wiley and Sons, 684 pp.

Zrnić, D. S., 1977: Spectral moment estimates from correlated pulse pairs. IEEE Trans. Aero. Elec. Sys., AES-13, 344–354.